Electrical properties of *p*-type Zn:Ga_2O_3 thin films

Ekaterine Chikoidze*[1], Corinne Sartel[1], H. Yamanno[2], Zeyu Chi[1], Guillaume Bouchez[1],
François Jomard[1], Vincent Sallet[1], Gérard Guillot[3], Kamel Boukheddaden[1],
Amador Pérez-Tomás[4], Tamar Tchelidze[5], Yves Dumont[1]

[1]Groupe d'Etude de la Matière Condensée (GEMaC), Université Paris-Saclay,
UVSQ – CNRS, 45 Av. des Etats-Unis, 78035 Versailles Cedex, France

[2]Department for Integrated Sensor Systems, Danube University Krems, 3500 Krems, Austria

[3]Univ. Lyon, CNRS, ECL, UCBL, INSA Lyon, CPE, Institut des Nanotechnologies de Lyon (INL-UMR5270),
69621 Villeurbanne Cedex, France

[4]Catalan Institute of Nanoscience and Nanotechnology (ICN2), CSIC and The Barcelona Institute of Science and Technology, Barcelona, Spain

[5]Faculty of Exact and Natural Science, Department of Physics, Ivane Javakhishvili Tbilisi State University, 3 Av. Tchavtchavadze, 0179 Tbilisi, Georgia

*Ekaterine Chikoidze: ekaterine.chikoidze@uvsq.fr

Key words: Gallium Oxide; acceptor doping; p type conductivity; Schottky diode simulation;

Abstract:

Ultra-wide bandgap Gallium oxide (~5 eV) has emerged as a novel semiconductor platform for extending the current limits of power electronics and deep ultraviolet optoelectronics at a predicted fraction of cost. Finding effective acceptor dopant for Gallium Oxide is a hot issue. One of the element which quite often is considered as a potential candidate is zinc. A number of experimental works have reported the signature of Zn-acceptor, but the direct evidence of hole conductivity were missing. In this work p type Zn doped Ga_2O_3 thin films were grown by MOCVD technique on sapphire substrate, by Hall Effect measurements it was determined Zn related acceptor level ionization energy as 0.77eV. Additionally we have carrier out the study regarding application of Zn:Ga_2O_3 as a guard ring material for Schottky diode structure.

I. INTRODUCTION

Ga_2O_3 (bandgap Eg~5 eV) is a representative ultra-wide bandgap (UWBG) oxide semiconductor that has attracted considerable interests owing to its unique combination of material properties, availability in large single crystals (at relatively low cost), heteroepitaxy developments onto cheap substrates (such as sapphire or silicon), tunable *n*-type conductivity, and ultra-high breakdown electrical field [1]. These properties make the material very attractive for deep ultraviolet optoelectronics and power electronics [1,2]. Combined with a number of technological breakthroughs, including the development of large commercial single crystals substrates and the demonstration of *n*-type conductivity tunable in a wide range with reasonable electron mobilities, Ga_2O_3 has improved potential for use in power electronics with reduced energy consumption and costs. It is also suitable for the next generation optoelectronic devices operating at shorter wavebands, because it has the widest bandgap among Transparent Conducting Oxides (TCOs) [3].

Finding effective acceptor dopant for Gallium Oxide is a hot issue. One of the element which quite often is considered as a potential candidate is zinc. Zinc (Zn) as a group 2 element is expected to be a good candidate as an acceptor in Ga_2O_3. Regarding the crystallographic structure of β-Ga_2O_3, there are two distinct Ga sites for Zn labelled Zn_{Ga1} and Zn_{Ga2} with the respectively tetrahedral and octahedral environments with expected different ionization energies [4]. However, due to its smaller atomic radius (137 pm) in comparison with that of Ga (153 pm), Zn can also occupy an interstitial position, thus acting as a donor. This amphoteric nature of Zn could be an origin of the possible so-called « *impurity auto-compensation effect* » [5]. A rather extensive number of theoretical studies have focused on understanding the microscopic mechanism of Zn doping in Ga_2O_3 during the last decade. (see *e.g.* [6,7]). Density functional theory (DFT) using local density approximation (LDA) and generalized gradient approximation (GGA) [8] has been widely employed [2]. A particular difficulty in β-Ga_2O_3 is the existence of two Ga lattice sites with different symmetries and related electronic properties and site-selective incorporation of the dopants. DFT seriously underestimates the bandgaps and the extent of charge localization at defects, thus predicting less accurate acceptor ionization energies. New approaches, including GGA+U (on-site coulomb interaction) and HSE (Heyd-Scuseria-Ernzerh) hybrid functional, have been developed and used to overcome deficiencies of DFT-LDA or GGA. However, due to the used calculation method, there is an

extensive dispersion of the obtained results in the literature. Some first studies claimed Zn to be a shallow acceptor at 0.070 eV and 0.050 eV for $ZnGa_1$ and $ZnGa_2$, respectively [6]. Kyrtsos *et al.* [7], in a later study, suggested that Zn in Ga sites have ionization energies varying from 0.35/0.27 eV to 1.39/1.22 eV for $ZnGa_1$/$ZnGa_2$ depending on the calculation methods. Finally, Lyons *et al.* [9], using hybrid DFT, who examined a large series of potential acceptors, including N, group 2 elements (Be, Mg, Ca, and Sr), and group 12 elements (Zn and Ca), concluded that all these elements are deep acceptors with levels higher than 1.3 eV.

Let us now summarize the main experimental results obtained on Zn doping. Very few experimental works focus on low doping cases (i.e., when incorporated Zn amount is less than 1%). Shrestha *et al.* [10] studied properties of 0.59% Zn doped Ga_2O_3 nano-porous layers for photo-induced hydrogen generation. It was concluded that the presence of a small amount of Zn doping in Ga_2O_3 can reduce trapping sites at the donor level under the conduction band, thereby increasing the mobility of electrons. On the other hand, Zinc doping also creates additional trapping sites as acceptor levels over the valence band, which hampers the activation of holes. Zn doping (up to 1 atomic % of zinc) on H_2O splitting was found to improve the photocatalytic activity, and it was attributed to the formation of an acceptor level, which enlarged the holes mobility and concentration [11]. Another study on monocrystalline Zn doped β-Ga_2O_3 nanowires/*n*-type β-Ga_2O_3 junction shows good rectifying behavior, suggesting that the Zn doped β-Ga_2O_3 nanowires are of *p*-type conductivity [12]. The cathodoluminescence spectra studies of Zn doped thin films suggest that the ionization energy of Zn could be in the range 0.25-0.5 eV, which is relatively shallow, still, the films remain highly resistive [13–15]. In ref 16 authors S.Baji et al, reported that Zn doping can decrease the resistivity of ALD deposited Ga_2O_3 films and can be used as an effective method for improving Ohmic contacts.[16]

Recent results obtained by EPR on bulk grown Zn doped Ga_2O_3 crystals identify the tetrahedral and octahedral sites of Zn_{Ga} with respectively thermal activation energy at 0.65 eV and 0.78 eV [17]. This work also confirms theoretical results based on total energy calculation showing that the octahedral site is predicted to be preferred by Zn [18]. The same result has been corroborated by another group [19], thus, unlike to other metal dopants, Zn has lower formation energy when replacing Ga in tetrahedral sites. **A number of experimental works have reported the signature of Zn-acceptor, but the direct evidence of hole conductivity is still missing**. **The objective of this work was the growth of p type Zn doped Ga_2O_3 thin films, determination of Zn related**

acceptor level ionization energy and study of its application as a guard ring material for Schottky diode structure.

II. CALCULATIONS AND EXPERIMENTAL

A. *Thermodynemic analysis*

It has been shown by thermodynamic analysis of point defects, that the window (pressure, temperature, Zn concentration) for the realization of Zn impurity controlled conductivity in Ga_2O_3 is very narrow. [5] The reason for the rather narrow range is the auto-compensation effect. In other words, Zn can play as an acceptor (Zn_{Ga}) as a donor (Zn_i) role. We have shown previously that when incorporated amount of Zn is around $10^{19}cm^{-3}$ this effect takes place, However it may be used to further increasing the Ga_2O_3's electrical breakdown field up to the ultra-high value beyond 13 MV/cm. [5]
In the present work our goal was to identify the window (growth temperature, pressure, Zn concentration) within which Zn related impurity hole conductivity can be realized in Ga_2O_3. From the thermodynamical point of view, using Kroger-Vink notations, the equilibrium relationships with the corresponding mass action laws are considered.See details in [5]. We calculated the concentration of defects for a several temperatures and a total pressure (30 torr) in the chamber reactor (these are the parameters we use in the experiment) versus Zn total concentration. Differently from our previous estimations, the defect creation enthalpies and defect ionization energies were adjusted to be more precise. The enthalpy of the transfer of Zn atoms from substitutional to the interstitial position is taken equal to the enthalpy of creation Frenkel pair in ZnO, as in Zn_{Ga} substitutional impurity Zn atoms are in chemical bond with oxygen ligands. The ionization energy of substitutional Zn atom is estimated in the frame of hydrogen atom model (in our previous calculations experimental data, were used). [5] The effect of Zn incorporation can give three different regions: (I) The range of *native conductivity* – in this range, the total concentration of Zn is deficient and dominant species are one-charged intrinsic acceptors $V_{Ga}^{/}$ and holes. (II) The range of *impurity p-conductivity* – with the increase of Zn concentration, Ga vacancies might be occupied with Zn atoms; so $[Zn_{Ga}^{-}] = p$. (III) the range of *impurity auto-compensation* – where

dominant species (point defects) are Zn_{Ga}^{-} and Zn_{i}^{+}. Fig. 1 shows Zn concentration versus temperature and three different regions of possible conductivity/compensation type.

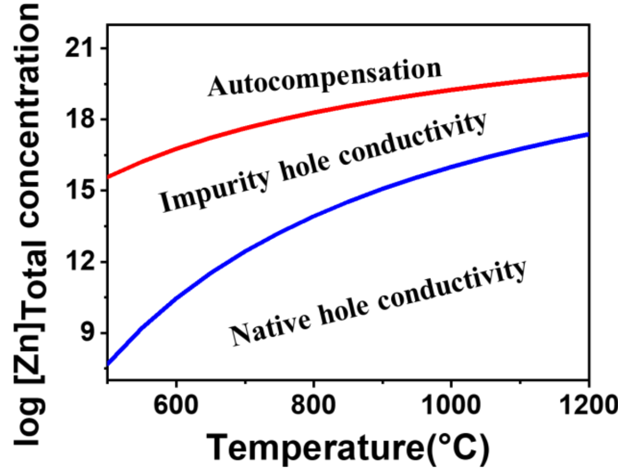

Fig. 1. Phase diagram: Incorporated Zn concentration versus temperature of intrinsic, impurity *p*-type, and impurity auto-compensation regions, with boundary curves (red and blue) for P_{tot} = 30 torr.

B. Zn:Ga₂O₃ epilayers

To achieve low levels of residual impurities, the chosen growth MOCVD (Metalorganic Chemical Vapour deposition) technique seems the most suitable. For example, the highest purity of *n*-type β-Ga_2O_3 (lower background donor concentration of 8×10^{14} cm^{-3}) thin films has been achieved by MOCVD growth [20], while semi-insulating *p*-type β-Ga_2O_3 have also been grown by the MOCVD technique [21]. In general, MOCVD is considered as the technique of choice for the growth of high purity, compensation free, thick β-Ga_2O_3 epilayers and their doping. Since 2018, the authors have already well-established experience of the growth of undoped *p*-type β-Ga_2O_3 epilayers on sapphire and silicon substrates. It is important to underline that doping by Zn is realized for the samples which are grown in the conditions assuring native hole conductivity originating from gallium vacancies [22]. In the present work, samples were grown at 775°C to be in the condition of realization of impurity conduction, according to thermodynamic analysis (Fig.1). From secondary

ion mass spectroscopy (SIMS) measurement, the incorporated Zn concentration was estimated as 10^{16} cm^{-3}. X-ray diffraction scan for undoped and doped samples are very similar and corresponds to β-Ga_2O_3 material. Fig.2a. Optical transmittance for undoped and doped samples shows that they are highly transparent (up to 80%) within the VIS-NIR range (Fig. 2(b)). The absorption onset starts at ~4.6 eV, and the obtained bandgap energies by using the Tauc's relationship were estimated to be Eg = 5.0 eV for the samples

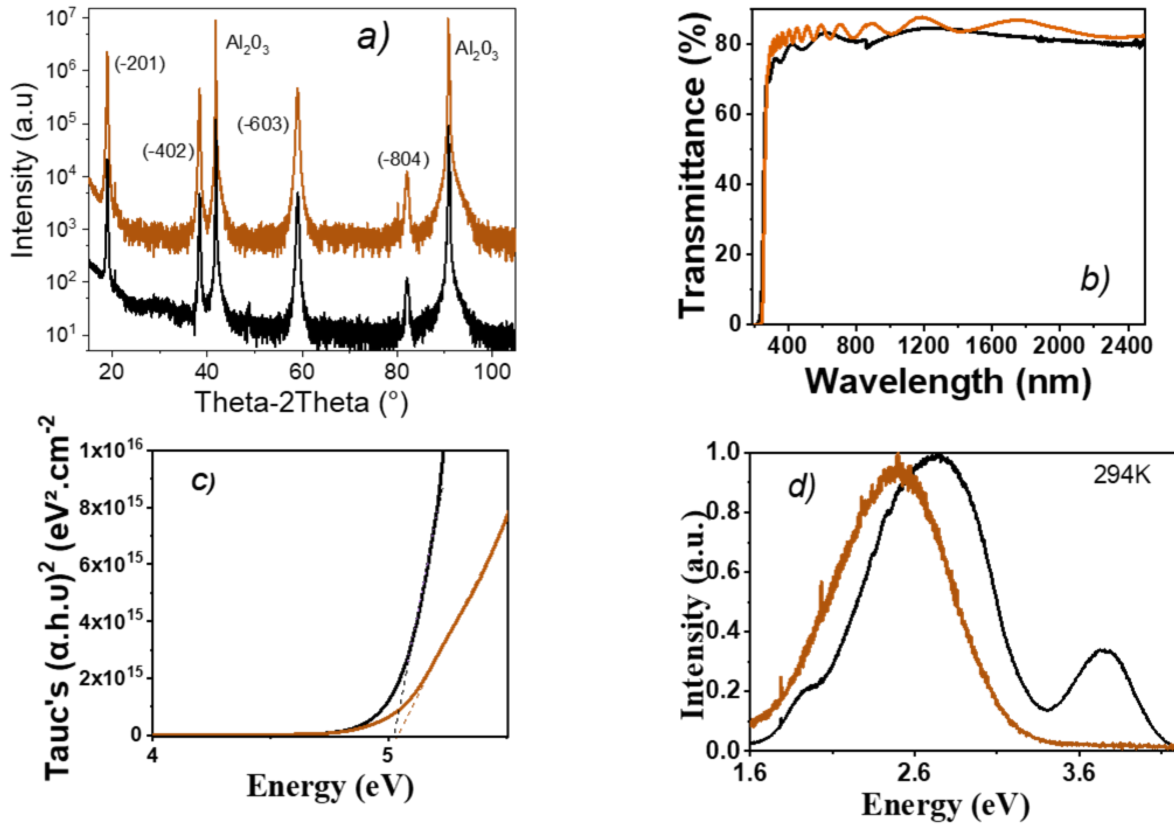

Fig. 2. Charcterization of undoped (black) and Zn: Ga_2O_3/sapphire (brown) thin films: a) X ray diffraction scans of undoped and Zn doped Ga_2O_3 epilayers growth on sapphire substrate. b) Optical transmittance. c) from Tauc's plot for bandgaps determination. Eg = 5.01 ± 0.14eV. d) Photoluminescence at, T = 294 K.

The photoluminescence emission spectra for Zn-doped and undoped p-type Ga_2O_3 excited with 266 nm wavelength at 294 K are shown in Fig. 2 (ds). Very interestingly, both samples have characteristic strong and broad emission (with Full Width at Half Maximum (FWHM) around 0.60 eV) centered at 2.5-2.6 eV. Indeed, this green emission has been already identified (though

much lower intensity) in the reference *p*-type undoped Ga_2O_3 samples and attributed to a native defect [22]. Because of the effective positive charge, the electron capture cross-section might be quite large, thus green emission would be a further signature of *p*-type Ga_2O_3. The native green emission has been found to remain invariant in intensity with Zn doping, similar effect has been observed in Zn doped Ga_2O_3 thin films grown by halide vapor epitaxy.[23] This emission is preliminarily ascribed to double-charged V_o oxygen vacancy, or V_o-V_{Ga} complex, which are abundant when free holes are present in the sample. A secondary ultraviolet (UV) emission peak at ~3.7 eV is visible for the undoped Ga_2O_3. This peak is ascribed to the electron transition from the V_{Ga} level, located at about ~1.2 eV from the valence band. The position of the UV emission level within the bandgap agree well with the ionization energy determined by electrical measurements for undoped Ga_2O_3 [21,22]. The disappearance of this band emission in doped samples might be related with Zn incorporation in V_{Ga} side.

III. RESULTS AND DISCUSSION

A. *Electrical transport properties*

To evaluate the electrical transport properties at different temperatures, Van der Pauw configuration was used and Ohmic electrical contacts were achieved by sintering an Ag paste. [20] Our interest was to study the sample with the lowest [Zn] = 10^{16} cm^{-3} concentration to determine the first time by electrical transport measurements the ionization energy of Zn related acceptor center. Fig. 3 (a) shows Van der Pauw resistivity temperature dependence in comparison with undoped *p*-type Ga_2O_3 sample. It is clear that Zn incorporation decrease resistivity: from $\rho_{500K} = 5 \times 10^6$ Ohm.cm to $\rho_{500K} = 1 \times 10^5$ Ohm.cm. Resistivity temperature behavior is classical of semiconducting type, decreasing with sample heating. Two conductivity regimes are distinguished corresponding to band activation ($T > 650$ K) and hopping mechanism at lower temperatures. Hall Effect measurements reveal that free hole concentration is increased in [Zn] = 10^{16} cm^{-3} doped sample by two orders of magnitude: p(850K) = 2×10^{15} cm^{-3} compared to p(850K) = 1×10^{13} cm^{-3} for the undoped sample (Fig. 3 (b)). The high-temperature region $T > 600$K corresponds to the band activation regime. This result is coherent what is seen in Fig. 1, that for such Zn concentration acceptor impurity conduction is prevalent. The temperature dependence of the holes concentration

was first analysed using the general expression of the electron concentration, n, in a partially compensated p-type semiconductor in the hypothesis of Boltzmann statistics and parabolic conduction band edge [24]:

$$\frac{g_d\, p(N_D + p)}{N_V\,(N_A - N_D - p)} = \exp\left(-\frac{E_A}{k_B T}\right) \text{ with } N_V = 2\left[\frac{2\pi m_v^* k_B T}{h^2}\right]^{3/2} \quad (1)$$

where N_D and N_A are the donor and acceptor concentrations, g_d the degeneracy factor for the acceptors, E_A the activation energy of the acceptor, k_B the Boltzmann constant, N_v the effective density of states in the valence band, h the Planck constant and m_v^* the equivalent density of states effective mass. E_A -activation energy which in this case equals the ionization energy E_i of acceptor level, is obtained from a linear regression on a $\ln(pT^{-3/2})$ vs $(1/T)$ plot (Fig.3 (c)). Following this, the activation energy of acceptor has been determined as E_i =1.1eV for undoped , as it's already reported by us related to V_{Ga} acceptor level and E_i= 0.77 eV for Zn doped sample. It is believed that Zn substitutes a gallium atom (Zn_{Ga}) thus creating an acceptor level at E_i= 0.77 eV which is completely consistent with the thermal activation energy of 0.65 eV and 0.78 eV determined by EPR spectroscopy for the two Zn_{Ga} sites [17].

Ga_2O_3 Hall hole mobilities are slightly decreased after Zn-incorporation (i.e., 10 cm^2/Vs for undoped and 7 cm^2/Vs for Zn:Ga_2O_3 being in both cases weakly depending on T (Fig.3 (d)). It is interesting to compare our results with a recently published report regarding electrical properties of [Zn] = 1.5×10^{18} cm^{-3} doped Ga_2O_3 bulk crystals: authors state that Zn introduces deep acceptor with trapping levels ~1.3 and ~0.9 eV above the valence band for one and two holes, respectively, and crystals were insulating [25]. It was supposed that such extremely high resistivity is most probably related to the number of high level unintentional compensating donor impurities presented in the crystal. [25]

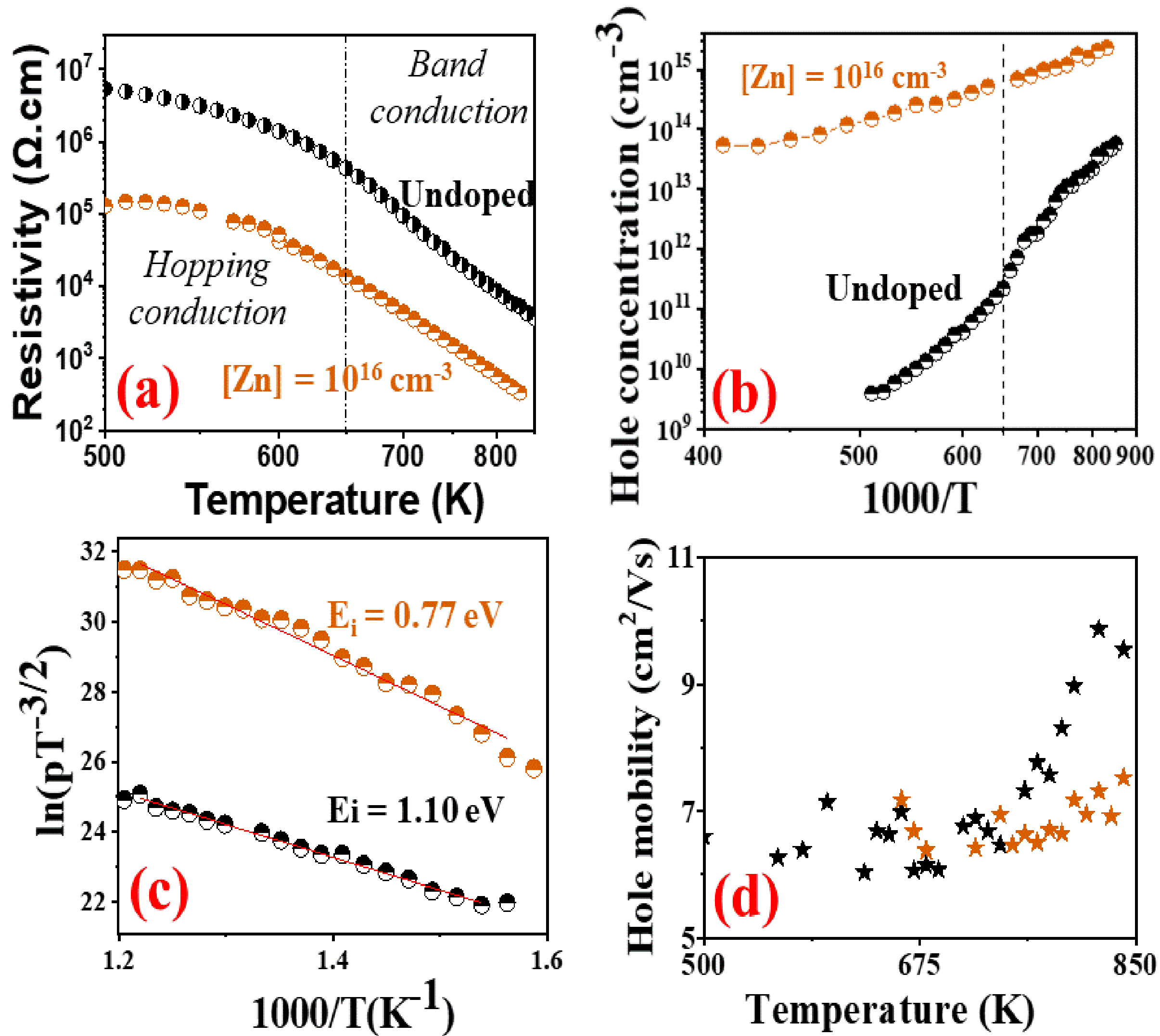

Fig. 3. a) Resistivity temperature dependence b) Hole concentration versus temperature c) ln($pT^{-3/2}$) temperature dependence and ionization energies d) Hall hole mobilities versus temperature for undoped (black stars) and Zn [1×10^{16} cm^{-3}] (red stars): Ga_2O_3 thin films.

B. Simulation: Zn:Ga_2O_3 as a protective guard ring

As it is demonstrated, Zn is undoubtfully a deep acceptor in Ga_2O_3 and indeed Zn doped Ga_2O_3 is considered having potentiality for being used as a semi-insulating substrate for power electronic devices. [26]

We have decided to investigate another possible application: if Zn doped gallium oxide can be used as a protective guard ring (GR) material for n type Ga_2O_3 based power Schottky diode. We have simulated the Schottky diode device structure, shown Figure.4, using Sentaurus device simulator. Pt (work function = 5.6 eV) was considered as a metal forming a Schottky contact with n-type Ga_2O_3. The following parameters for doping densities and ionization energies were used: N_D =1x10^{17} /cm^3, E_i=30 meV for n- Ga_2O_3 active layer and N_A=1x10^{19} /cm^3, E_i=0.77 eV for Zn: Ga_2O_3 GR layer.

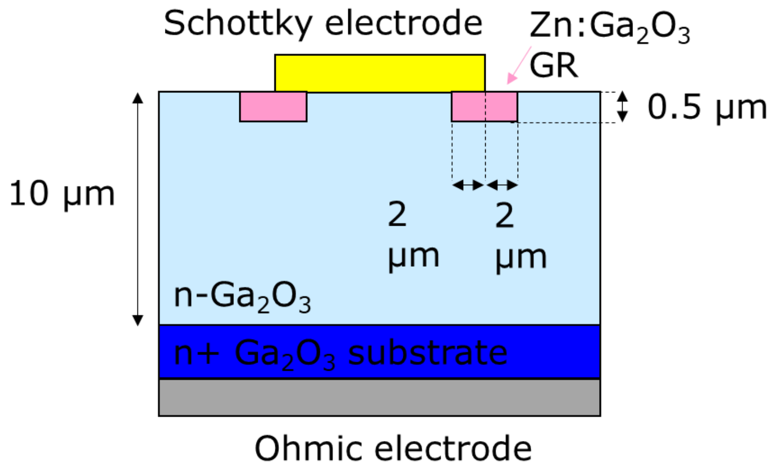

Figure 4. Schottky device structure used for simulation.

Figure 5 (a) shows the Current-voltage (I-V) reverse characteristics of device without and with GR. We obtain breakdown voltages as V_{br}=288 V for unprotected structure while with GR layer V_{br} =474 V. Figure 5(b)-(d) shows acceptor (Zn) doped area and the electric field distribution at 250 V without and with GR. The horizontal axis shows the distance from the edge of Schottky electrode and the vertical axis shows the distance from Ga_2O_3 surface. Without GR, the high electric field is observed at the edge of Schottky electrode. On the other hand with GR, there is no high electric field around the edge of electrode and high field is observed at the interface between

n-type Ga_2O_3 and p-type Zn:Ga_2O_3 GR layer. It means that we can prevent the high electric field at the weak metal/semiconductor interface by such GR. This is interesting and encouraging result for potential use of deep Zn acceptor dopant in Ga_2O_3 (E_i = 0.77 eV), for improvement of the breakdown voltage capability of Schottky diode.

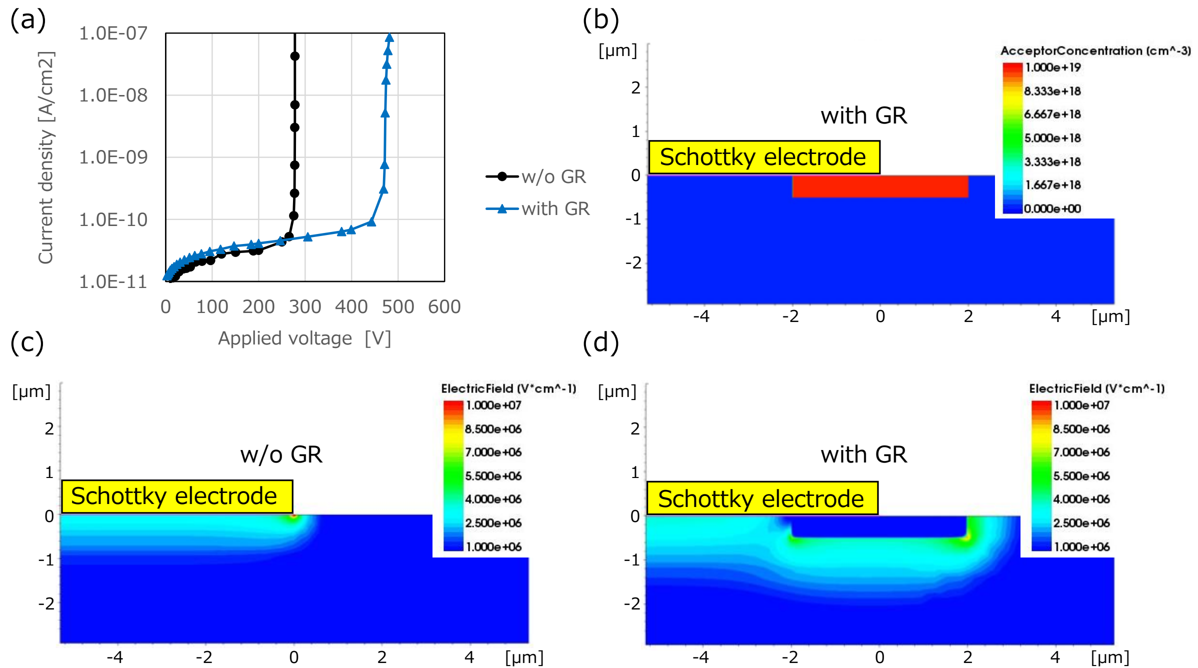

Figure 5. (a) Reverse I-V characteristics without and with GR of Schottky device structure, (b) Zn doping profile, (c) Electric field distribution at 250 V without GR, (d) Electric field distribution at 250 V with GR.

IV. SUMMARY AND CONCLUSIONS

There are number of reports claiming that Zn can play the role of acceptor in gallium Oxide. Though, up today no evidence was reported of Zn related electrical activity, leading p type conduction. In the present work the first time we demonstrate by Hall Effect measurements that Zn on Ga site introduces deep acceptor level in the gap: with 0.77eV ionization energy and can be a source of free holes. Evidently, being deep acceptor, electrical activity of this dopant can be important only at high temperatures, which make Zn as a mono-dopant not very suitable for room temperature hole conduction realization in Ga_2O_3. Other hand, we have tried to evaluate the effect of Zn: Ga_2O_3 on the breakdown capability of Schottky diode, if using it as a guard ring structure.

According to our simulations such GR can prevent the high electric field at the weak metal/semiconductor interface.

Experiment methods

The Zn:Ga_2O_3 samples were grown in a RF-heated horizontal MOCVD reactor on sapphire (Al_2O_3) substrates. during the growth, the flow rate of the gallium precursors and oxygen were kept at 6 μmol/min and 600 sccm respectively. The growth temperature, pressure and time were set at 775°C, 30 torr. The TMGa and DEZn bubbler temperatures were fixed at -10°C and 0°C, respectively. The DEZn flow was varied as 0; 1.6; μmol/min. Secondary-ion mass spectrometry (SIMS) using a Cameca IMS 4f equipment was performed onto the samples to measure the depth distribution of Zn dopant.

Hall Effect measurements has been carried out by home built high impedance high temperature set up in Van der Pauw configuration. High temperature Ohmic contacts were prepared by silver paint at the four corners of the sample. Hall effect measurements were performed in a Van der Pauw configuration in the temperature range of 300K to 850K and for magnetic fields perpendicular to the film plane varying from -1.6 T to 1.6 T, using a high impedance measurement set-up which was custom designed for measurement of high resistance samples. Optical transmittance spectrum was measured in 200-2000 nm spectral range with a Perklin Elmer 9 spectrophotometer.

Photoluminescence set up consists with YAG laser with continuous emission of 266nm (CryLaS FQCW266-10-C) which was used as a excitation source. Collected signals were analysed by spectrometer (Princeton Instrument IsoPlane 320).

The thermodynamic equilibrium in the Zn:Ga_2O_3 (crystal)–O_2 (gas) system was modeled in order to define the dependence of point defects, charge carriers on temperature and oxygen partial pressure in the surrounding atmosphere. Knowing these dependences, the treatment temperature and oxygen pressure, for which creation of compensating donor defects are suppressed and acceptors and holes become dominant species can be determined. The analysis was made using the Kroger method of quasi-chemical equations [27].

Device simulations were performed by Sentaurus device simulator with the Chynoweth model.[28] As the Chynoweth parameters for the impact ionization coefficient $\alpha(E) = a*\exp(-b/E)$, where E is the electric field, we have used a = 0.706×10^6 /cm and b = 2.10×10^7 V/cm. [21,29] Electron's and hole's mobility were set based on some experimental results.[30]

ACKNOWLEDGMENTS

The ICN2 is funded by the CERCA programme / Generalitat de Catalunya and by the Severo Ochoa programme of the Spanish Ministry of Economy, Industry and Competitiveness (MINECO, grant no. SEV-2017-0706). GEMaC colleagues acknowledge financial support of French National Agency of Research (ANR), project "GOPOWER",CE-50 N0015-01

CONFLICT OF INTERESTS

The authors have no conflicts to disclose.

DATA AVAILABILITY

The data that support the findings of this study are available from the corresponding author upon reasonable request.

REFERENCES

[1] S.J. Pearton, F. Ren, M. Tadjer, and J. Kim, Journal of Applied Physics **124**, 220901 (2018).
[2] J. Zhang, J. Shi, D.-C. Qi, L. Chen, and K.H.L. Zhang, APL Materials **8**, 020906 (2020).
[3] J. Zhang, C. Xia, Q. Deng, W. Xu, H. Shi, F. Wu, and J. Xu, Journal of Physics and Chemistry of Solids **67**, 1656 (2006).
[4] J. Åhman, G. Svensson, and J. Albertsson, Acta Cryst C **52**, 1336 (1996).
[5] E. Chikoidze, T. Tchelidze, C. Sartel, Z. Chi, R. Kabouche, I. Madaci, C. Rubio, H. Mohamed, V. Sallet, F. Medjdoub, A. Perez-Tomas, and Y. Dumont, Materials Today Physics **15**, 100263 (2020).
[6] C. Li, J.-L. Yan, L.-Y. Zhang, and G. Zhao, Chinese Phys. B **21**, 127104 (2012).
[7] A. Kyrtsos, M. Matsubara, and E. Bellotti, Appl. Phys. Lett. **112**, 032108 (2018).
[8] C.Y. Yu, X.J. Liu, J. Lu, G.P. Zheng, and C.T. Liu, Sci Rep **3**, 2124 (2013).
[9] J.L. Lyons, Semicond. Sci. Technol. **33**, 05LT02 (2018).
[10] N.K. Shrestha, K. Lee, R. Kirchgeorg, R. Hahn, and P. Schmuki, Electrochemistry Communications **35**, 112 (2013).
[11] Y. Sakata, Y. Matsuda, T. Yanagida, K. Hirata, H. Imamura, and K. Teramura, Catalysis Letters **125**, 22 (2008).

[12] Q. Feng, J. Liu, Y. Yang, D. Pan, Y. Xing, X. Shi, X. Xia, and H. Liang, Journal of Alloys and Compounds **687**, 964 (2016).
[13] X.H. Wang, F.B. Zhang, K. Saito, T. Tanaka, M. Nishio, and Q.X. Guo, Journal of Physics and Chemistry of Solids **75**, 1201 (2014).
[14] F. Alema, B. Hertog, O. Ledyaev, D. Volovik, G. Thoma, R. Miller, A. Osinsky, P. Mukhopadhyay, S. Bakhshi, H. Ali, and W.V. Schoenfeld, Phys. Status Solidi A **214**, 1600688 (2017).
[15] F. Alema, B. Hertog, A. Osinsky, P. Mukhopadhyay, M. Toporkov, and W.V. Schoenfeld, Journal of Crystal Growth **475**, 77 (2017).
[16] Z. Baji, I. Cora, Z.E. Horváth, E. Agócs, and Z. Szabó, Journal of Vacuum Science & Technology A **39**, 032411 (2021).
[17] T.D. Gustafson, J. Jesenovec, C.A. Lenyk, N.C. Giles, J.S. McCloy, M.D. McCluskey, and L.E. Halliburton, Journal of Applied Physics **129**, 155701 (2021).
[18] D. Skachkov and W.R.L. Lambrecht, Appl. Phys. Lett. **114**, 202102 (2019).
[19] C. Zhang, F. Liao, X. Liang, H. Gong, Q. Liu, L. Li, X. Qin, X. Huang, and C. Huang, Physica B: Condensed Matter **562**, 124 (2019).
[20] M.J. Tadjer, F. Alema, A. Osinsky, M.A. Mastro, N. Nepal, J.M. Woodward, R.L. Myers-Ward, E.R. Glaser, J.A. Freitas, A.G. Jacobs, J.C. Gallagher, A.L. Mock, D.J. Pennachio, J. Hajzus, M. Ebrish, T.J. Anderson, K.D. Hobart, J.K. Hite, and C.R. Eddy Jr., J. Phys. D: Appl. Phys. **54**, 034005 (2021).
[21] E. Chikoidze, C. Sartel, H. Mohamed, I. Madaci, T. Tchelidze, M. Modreanu, P. Vales-Castro, C. Rubio, C. Arnold, V. Sallet, Y. Dumont, and A. Perez-Tomas, Journal of Materials Chemistry C **7**, 10231 (2019).
[22] E. Chikoidze, A. Fellous, A. Perez-Tomas, G. Sauthier, T. Tchelidze, C. Ton-That, T.T. Huynh, M. Phillips, S. Russell, M. Jennings, B. Berini, F. Jomard, and Y. Dumont, Materials Today Physics **3**, 118 (2017).
[23] G. Pozina, C.-W. Hsu, N. Abrikossova, and C. Hemmingsson, Phys. Status Solidi A 2100486 (2021).
[24] J.S. Blakemore, *Semiconductor Statistics* (Courier Corporation, 2002).
[25] J. Jesenovec, J. Varley, S.E. Karcher, and J.S. McCloy, Journal of Applied Physics **129**, 225702 (2021).
[26] C. Pansegrau, J. Jesenovec, J.S. McCloy, and M.D. McCluskey, Appl. Phys. Lett. **119**, 102104 (2021).
[27] *F.A. Kroger, "The Chemistry of Imperfect Crystals", North-Holland Publishing Company, Amsterdam, 1964, Pp.1039* (n.d.).
[28] https://www.synopsys.com/silicon/tcad/device-simulation/sentaurus-device.htm
[29] K. Ghosh, and U. Singisetti, Journal of Applied Physics **124**, 085707 (2018).

[30] J. Zhang, J. Shi, D.-C. Qi, L. Chen, and K. H. L. Zhang, APL Materials **8**, 020906 (2020).